D-NMR study on pores of the activated carbon fiber electrode for EDLC with inorganic electrolyte

Sang-Ick Lee*, Mitani Satoshi, Seong-Ho Yoon, Yozo Korai, Koji Saito, Isao Mochida

Institute for materials chemistry and engineering, Kasuga, Fukuoka 816-8580, Japan

*Corresponding author e-mail; silee9@asem.kyushu-u.ac.jp

1. Introduction

The electric double-layer capacitor (EDLC) using activated carbon as electrodes has been recognized as an efficient storage device for the electric power because of its better rate capability and longer cycle life as compared to secondary batteries in spite of its low energy density [1,2]. Recently new applications utilizing such performances have been attempted as an energy storage device for electric vehicle or pulse-current supply. In order to meet the specification for new application, it is necessary for particular activated carbon to have higher energy density per weight or volume than the conventional one.

Activated carbons with the specific surface areas beyond 2000m^2/g have been prepared from the various carbon precursors by chemical or gas-phase activation, resulting in high capacitance per weight [3-5]. Nevertheless, they still suffer from low electrode density and capacitance per volume which lower the compactness of EDLC. Their effectiveness per surface area and pore volume stays rather low. Many researchers have correlated the capacitance with one of carbon properties to find the dominant factor which may influence the capacitance directly, although their success was very limited [6-8].

In the present study, adsorption of H_2SO_4 over this series of ACFs was measured by both solid state ^{2}H-NMR to clarify the state of its adsorption related to the capacitance. The H_2SO_4 electrolyte can be present on the pore wall, in the pore or on the external surface of ACF. Such states of H_2SO_4 in the electrode can be distinguished with solid state ^{2}H-NMR in terms of their chemical shift and line width by magic angle spin technique. Solid state NMR is a sole and powerful method to solve the chemical and dynamic behaviors of H_2SO_4 adsorbed on the

wall of the pore [9-11].

2. Experimental

2.1. Material. ACFs with the variable surface areas were supplied by Osaka Gas Co. Elemental analyses, surface area, and pore volume of the ACFs are summarized in Table 1.

2.2. Measurement of Capacitance. Capacitance in inorganic electrolyte (30% H_2SO_4) was measured in a beaker-type two electrode cell, and its current collector was Pt. The test cell consisted of a pair of electrodes and immersed in 30% sulfuric acid under vacuum for 3h. The electrode was composed of ACF (80% by weight), polytetrafluoroethylene (PTFE) as a binder (10%), and carbon black as an electric conductor (10%). The test cell was charged to 0.9V at a constant current-constant voltage, and then discharged at a constant current to 0V. Double layer capacitance was calculated from the time period of voltage change between 0.72 and 0.36V.

Capacitance using organic electrolyte was measured in a coin-type two electrode cell. The test cell consisted of a pair of electrodes and immersed in 1M tetraethylammonium tetrafluoroborate / propylene carbonate. The electrode had the same composition as that of electrode in the inorganic capacitor. The test cell was charged to 2.7V at a constant current-constant voltage, and then discharged at a constant current to 0V. Double layer capacitance was calculated from the time period of voltage change between 2.16 and 1.08V. It must be emphasized that the capacitance described here is measured by two-electrode galvanostatic mode and that capacitances per weight and volume were calculated on the basis of the electrode.

2.3. ^{2}H-NMR. Deuterated sulfuric acid (D_2SO_4, Aldrich Chemical Co.) was diluted to 30% in deuterium oxide. The dilute D_2SO_4 was soaked into the ACFs at room temperature under vacuum for 3h. Wet ACFs were placed between the filter paper and tapped to remove the excess of D_2SO_4 present on the outer surface of ACFs. The ^{2}H-NMR spectra were obtained at 400 MHz using JNM-ECA400 (Jeol) with a 6mm magic angle spinning (MAS) probe.

^{2}H-NMR spectra for each ACF was obtained from the static state to MAS of 4 kHz. Chemical shifts are relative to the liquid-phase 30% D_2SO_4 set at 0 ppm.

3. Results

3.1. Capacitance of ACFs. Capacitances of ACFs in the inorganic capacitor are summarized in Table 1. Capacitance per weight increased from 33F/g for OG5A to 43F/g for OG20A according to their surface areas. In contrast, their capacitances per volume decreased from 29F/ml for OG5A to 21F/ml for OG20A. OG5A and 7A in the organic capacitor showed very low capacitance per weight, whereas OG20A showed the largest capacitance per weight of 29F/g, while OG10A of the moderate surface area did the largest capacitance per volume of 17F/ml.

Table 1. Properties and capacitances of ACFs

ACFs	SA[1]	PV[2]	Inorganic		Organic		PWHH[3]	CS[4]
	(m^2/g)	(ml/g)	F/g	F/ml	F/g	F/ml	(Hz)	(ppm)
OG5A	480	0.25	33	29	5	4	457	-4.7
OG 7A	690	0.36	32	28	3	3	461	-9.9
OG 10A	1060	0.55	35	23	26	17	79	-3.1
OG 15A	1160	0.57	38	24	25	16	75	-3.4
OG 20A	2140	1.05	43	21	29	14	66	-2.7

[1]Specific surface area; [2]specific pore volume; [3]peak width at half height; [4]chemical shift

Figure 1 shows the comparison between capacitance per weight and the surface area of ACFs in the inorganic capacitor. The capacitance per weight of the ACFs in the inorganic capacitor was linearly correlated with their specific surface areas. However, the correlation line of very small slope did not cross the zero point, indicating that the surfaces of ACFs did not equally contribute to the capacitance. Capacitance per surface area of ACF was the largest with OG5A and 7A of the smaller surface area, suggesting that the surface of their pore walls

is more effective than those of ACFs with larger surface area.

Figure 1 also includes the relationship between organic capacitance per weight and surface area of ACFs. The capacitance per weight of the ACFs was linearly correlated to their surface area below 1000m^2/g, being saturated around the surface area of 1000m^2/g (OG10A). OG10A showed the largest effectiveness of its surface in the organic capacitance among ACFs in the present study.

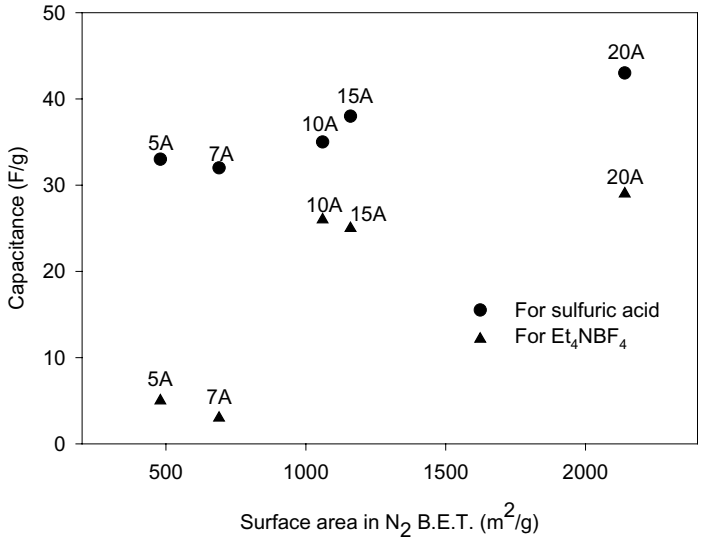

Figure 1. Comparison of capacitance per weight with surface area.

3.2. ^{2}H-NMR Spectra of D_2SO_4 Adsorbed on ACFs. Figure 2 shows solid state ^{2}H-NMR spectra of OG5A impregnated with 30% D_2SO_4 as the function of the rate of MAS. Without MAS, a very broad peak centered at 0ppm was observed. All spectra at various MAS showed a sharp peak at 0ppm and broad one at about -5ppm, except for the spectrum at 1.6 kHz which provided two peaks at around 0ppm. The chemical shift of the D_2O in ^{2}H-NMR spectra has been reported to shift to low field by the shielding by π-electrons on the graphene planes of activated carbon [12,13]. The adsorption of D_2SO_4 restricted its motion, broadening its peak. Therefore, in the present study, the sharp peak at 0ppm and broad one at about -5ppm are assigned to the non-adsorbed D_2SO_4 and the fixed D_2SO_4 on the pore wall, respectively. The non-adsorbed D_2SO_4 included that in the pore and on the outer surface. A particular MAS of 1.6 kHz split the peak at about 0ppm into two at -0.7 and 0.4 ppm, respectively. The lower

field peak can be assigned to D_2SO_4 in the pore since D_2SO_4 in the pore must be influenced more effectively by the graphene sheet of pore wall than that on the outer surface.

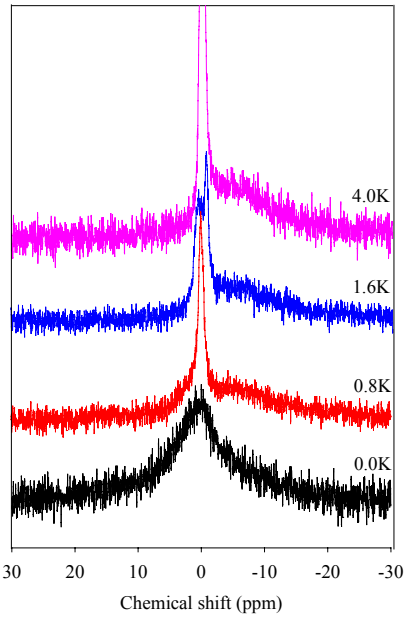

Figure 2. ^{2}H-NMR spectra of OG5A impregnated with 30wt% D_2SO_4.

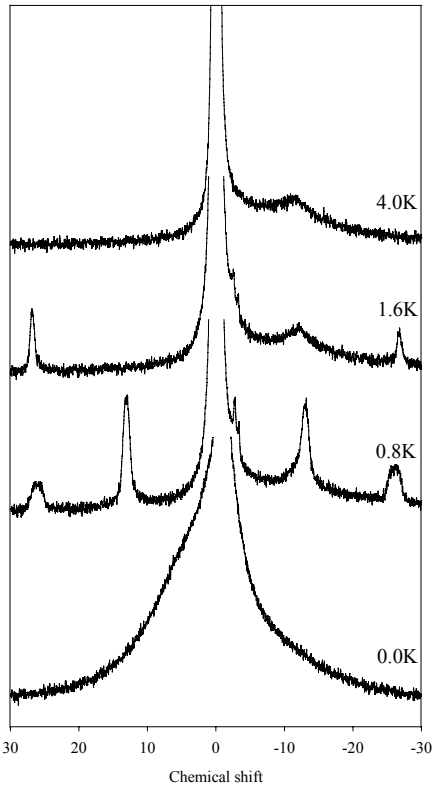

Figure 3. ^{2}H-NMR spectra of OG7A impregnated with 30wt% D_2SO_4.

Figure 3 shows ^{2}H-NMR spectra of OG7A impregnated with 30% D_2SO_4 as the function of the rate of MAS. In contrast to those of OG5A, all spectra under MAS showed strong side bands at the center of the peak at 0ppm. A particular orientation of the trapped D_2SO_4 causing anisotropic dipole like crystal in this particular pore may provide the side bands which were shifted further by rapid MAS. No peak separation was observed at about 0ppm with this ACF according to the increase of MAS as shown in Figure 3. A broad but very definite peak appeared at about 10ppm, being assigned to the fixed D_2SO_4 on the pore wall.

^{2}H-NMR spectra of OG10A, 15A, and 20A impregnated with 30wt% D_2SO_4 are shown in Figure 4. OG10A showed the peak with a shoulder at about 0ppm when the rate of MAS was 0.8 kHz. The shoulder peak was merged on the main peak by MAS above 1.6 kHz. The broad

peak due to the fixed D_2SO_4 was clearly observed at -3.1ppm above 0.8 kHz MAS. The broad peak of the fixed one remained separated from the peak of 0ppm at MAS of 4.0 kHz. The exchange between the non-adsorbed D_2SO_4 over the outer surface and the trapped D_2SO_4 in the pore is suggested by separated peaks at 0.8 kHz, whereas the exchange between the trapped and the fixed D_2SO_4 on the pore wall was not verified by MAS of 4.0 kHz.

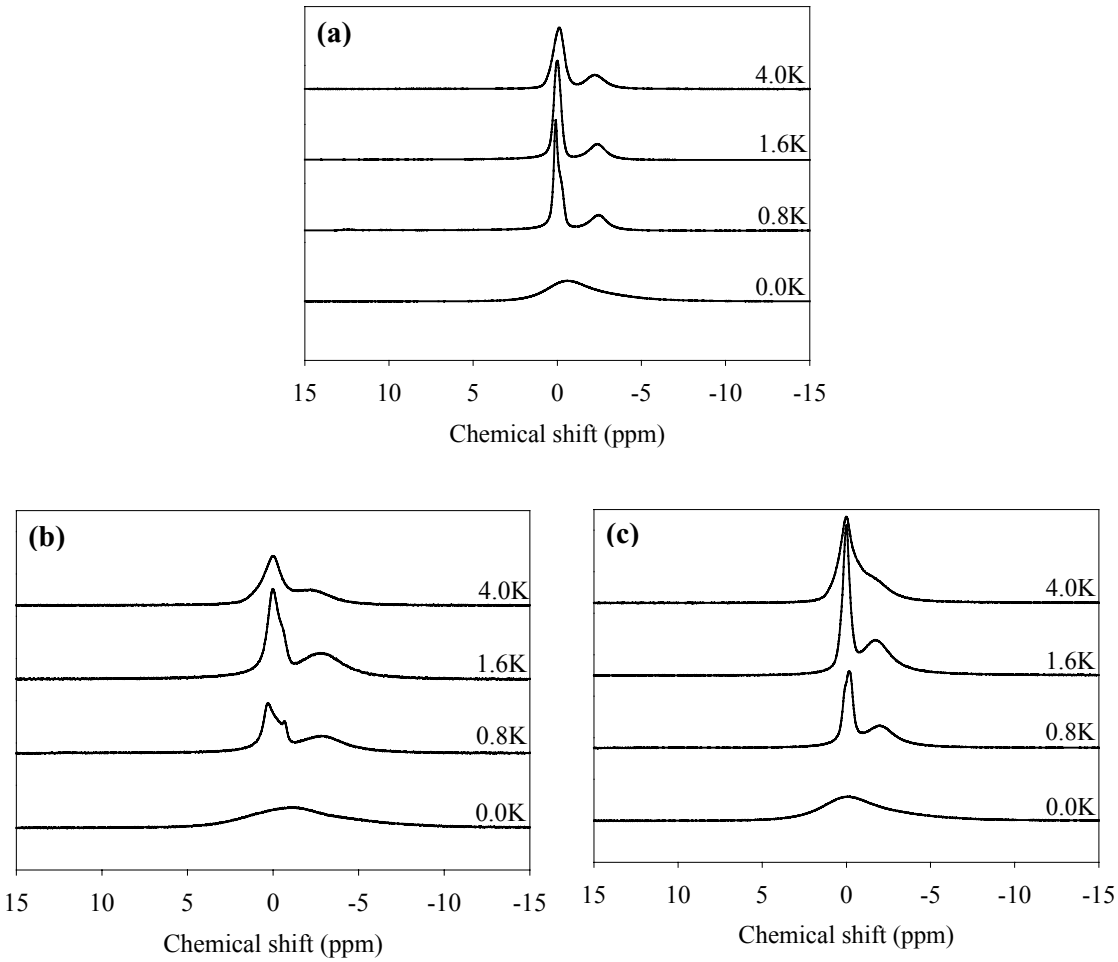

Figure 4. ^{2}H-NMR spectra of OG10A (a), 15A (b), and 20A (c) impregnated with 30wt% D_2SO_4.

OG15A showed the separated peaks around 0ppm when MAS were at 0.8 and 1.6 kHz. A broad peak was definitely observed at -3ppm by MAS of 0.8 kHz. The overlapping of two peaks observed by 4.0 kHz means the beginning of exchange between two D2SO4 species such as the trapped and the fixed D_2SO_4. An averaging effect of two-state D_2SO_4's allows

higher field shift of the fixed D_2SO_4. ^{2}H-NMR spectra of OG20A showed similar trends to those of OG15A except for more marked overlapping of the peaks at 0 and 2.7ppm.

The values of chemical shift in ppm and peak width at half height in Hz of the respective peaks are summarized in Table 1. OG5A and 7A showed the peaks of larger width at about -5ppm and -10ppm, respectively, while OG10, 15 and 20A had the peaks of much narrower width around -3ppm. In other words, OG5A and 7A restricted more strongly the motion of the fixed D_2SO_4 on their pore wall of ACFs, and thus chemical shifts by the graphene planes are larger than those of OG10A, 15A and 20A. D_2SO_4 in OG10A must be noted to behave differently from those of OG15 and 20A in terms of peak merging at rapid MAS.

4. Discussion

4.1. Capacitance *versus* Surface Area. Figure 1 compares the capacitances and surface areas of a series of pitch ACFs. The capacitance of ACFs in inorganic capacitor depends very slightly on their surface areas. OG5A ($480m^2/g$) and OG20A ($2140m^2/g$) showed two-electrode capacitances of 33 and 43F/g, respectively. The capacitances per surface area were calculated as 0.07 and $0.02F/m^2$ with OG5A and 20A, respectively. OG5A had the largest capacitance per volume of 29F/ml..

The function of ACF as the electrode material for the inorganic capacitor is very different from that for the organic capacitor using Et_4NBF_4 as the electrolyte. The quaternary ammonium salt such as Et_4NBF_4 has larger ionic and solvated diameters than those of H_2SO_4 in the inorganic capacitor. A better correlation between organic capacitance per weight and surface area of ACF was obtained in the present study. Nevertheless, capacitance per volume was the largest for OG10A with the moderate surface area, not with OG20A of the largest surface area. Such results strongly suggest that the surface area is not a sole factor for the capacitance of ACF. The factors of the effective surface which can contribute to the capacitance should be defined. Surface structure of the activated carbons must be evaluated to obtain their high capacitance especially per volume. The pore size has been recognized as an

important factor to explain the effectiveness of activated carbon since the electrolyte can not access too small pore, hence preventing it from forming a double layer on the pore wall. Larger electrolyte of Et_4NBF_4 may not be allowed to penetrate into the smaller pores of ACFs with smaller surface area. Such a comparative study using electrolytes with different sizes can be useful in determining what pore size is too small to access the organic electrolyte. However, this particular comparative study also fails to explain why OG5A of the smallest surface area is more effective in the inorganic capacitor than 20A with larger surface area. It is necessary to find out other influential factors to define the capacitance through the liquid-phase adsorption of H_2SO_4 on ACF.

4.2. H_2SO_4 Adsorbed on ACF. H_2SO_4 is found to be present in three states on ACF by ^{2}H-NMR. One is adsorbed on the surface of the pore wall in the ACF, another is trapped in the pores of the ACF, and the last one is present over the outer surface.

The chemical shift and line width of ^{2}H-NMR spectrum reflect the states of adsorbed H_2SO_4. OG5A and 7A showed stronger adsorption of H_2SO_4 on the pore wall, providing a peak of very broader line-shape and larger chemical shift (-4.7 and -9.9ppm, respectively). In contrast to OG5A and 7A, OG10, 15 and 20A showed weak adsorption of H_2SO_4, as indicated by the narrow line shape and small chemical shift (about -3ppm). Such chemical shift and line width reflect the state of adsorbed H_2SO_4 which defines its contribution to EDLC performance. The exchange between H_2SO_4 adsorbed on the pore wall and trapped in the same pore can be found to weaken the adsorption of H_2SO_4 on the pore wall. Larger amount of H_2SO_4 in the pore must accelerate such an exchange of adsorbed H_2SO_4. Hence, H_2SO_4 adsorbed on the pore wall of the large pore can be averaged through the exchange with relatively free H_2SO_4 trapped in the same pore. The polarization of adsorbed species can be weakened by the exchange with less polarized H_2SO_4 in the pore.

Thus, the exchange between the adsorbed H_2SO_4 and the trapped H_2SO_4 in the same pore is assumed to play an unfavorable role to decrease the polarization of the adsorbed H_2SO_4,

which must reduce the capacitance of EDLC. Such exchange reduces more the polarization of the adsorbed H_2SO_4 when larger amount of free H_2SO_4 is present in the same pore. Hence, a larger pore of larger volume relative to its wall surface decreases the contribution of adsorbed H_2SO_4 species to EDLC. This is the case with OG10, 15 and 20A for the inorganic capacitor. The situation is similar with the organic capacitor. However the larger size of its electrolyte shifts the optimum pore structure to that of OG10A. Side band observed exclusively with H_2SO_4 on OG7A must be discussed. Side band is observed when magnetic species are arranged to show the particular anisotropy in their fixed state as observed like solid crystal. Hence, adsorption does not always show the side band. The side bands centered at 0ppm must reflect the whole H_2SO_4 in the pore. A state like an ice of H_2SO_4 aligned to show anisotropy can be assumed in the pore of the particular ACF, OG7A.

References

(1) Nishino, A. *J. Power Sources* **1996,** 60, 137.

(2) Christen, T.; Carlen M. W. *J. Power Sources* **2000,** 91, 210.

(3) Teng, H.; Chang, Y.; Hsieh, C. *Carbon* **2001,** 39, 1981.

(4) Endo, M.; Maeda, T.; Takeda, T.; Kim, Y. J.; Koshiba, K.; Hara, H.; Dresselhaus, M. S. *J. Electrochem. Soc.* **2001,** 148, A910.

(5) Nishino, A. *Technologies and Materials for EDLC and Electrochemical Supercapacitors*; Nishino, A., Naoi, K., Eds., CMC: Tokyo, 2003, pp 129-174.

(6) Tanahashi, I.; Yoshida, A.; Nishino, A. *Bull. Chem. Soc. Jpn.* **1990,** 63, 3611.

(7) Tanahashi, I.; Yoshida, A.; Nishino, A. *J. Electrochem. Soc.* **1990,** 137, 3052.

(8) Shi, H. *Electrochim. Acta* **1996,** 41, 1633.

(9) Takeuchi, M.; Koike, K.; Maruyama, T.; Mogami, A.; Okamura, M. *Denki Kagaku* **1998,** 66, 1311.

(10) Min, K. H.; Takimoto,Y.; Yamada, K.; Simoyana, T.; Yamamoto, K.; Yonemori, S.; Hiratsuka, K. *Fall Meeting of ECS*, San Francisco, 2001, Abstract No.283.

(11) Hayamizu, K.; Akiba, E. *Electrochemistry* **2003,** 71, 1052.

(12) Harris, R. K.; Thompson, T. V.; Forshaw, P.; Foley, N.; Thomas, K. M.; Norman, P. R.; Pottage, C. *Carbon* **1996,** 34, 1275.

(13) Heinen, A. W.; Peters, J. A.; Bekkum, H. *Appl. Cat. A: General* **2000,** 194-195, 193.